SUPPLEMENTARY TO BE NOT PUBLISHED

This appendix presents further empirical results and the document will be published in the Github.

G. Impact of AN on the I3D Feature Anomaly Localization

Fig. 16 depicts a 2D visualization of the extracted I3D features ($B = 5 \times D = 1024$) from a sample video. We selected the example video, where the VAD improves for $\mathcal{G}^{\text{a}}$ but $\mathcal{P}_4^{\text{a}}$, to demonstrate the smoothing effect of $\mathcal{G}$ filtering. The figures show the distinctness of anomaly and normal video frames after I3D feature extraction. The final VAD also depends on the relative importance of the features for the employed VAD model. The per-file $\text{AUC}_{\text{PEL4VAD}}$ achieves No-AN: 0.744, MASKED: 0.881, EDGED: 0.474, $\mathcal{G}^0$: 0.665, $\mathcal{G}^{\text{a}}$: 0.921, $\mathcal{G}^{\text{a}}_{\text{max}}$: 0.969, $\mathcal{P}_4^0$: 0.767, $\mathcal{P}_4^{\text{a}}$: 0.664, and $\mathcal{P}^{\text{a}}_{\text{max}}$: 0.919.

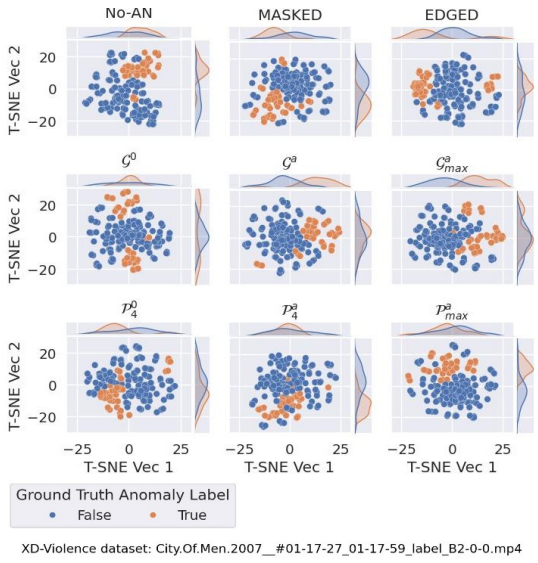

Fig. 16: Illustration anomaly localization robustness using 2D ($T \times 2$) T-SNE embedding of the video I3D features ($T \times B = 5 \times D = 1024$). The MASKED and $\mathcal{G}^{\text{a}}$ improve the clustering. The plots demonstrate the gain of $\mathcal{G}^{\text{a}}$ due to enhanced denoising, whereas EDGED and $\mathcal{P}_4^{\text{a}}$ add a slight perturbation that lowers the VAD.

H. Further Evaluation on Adaptive Scaling Hyperparameters

We present below further analysis on the hyperparameter of α_l in Eq. (12) and the adaptive scaling function in Eq. (10).

Fig. 17 presents the impact of α_l on PD and VAD. When α_l varies between 0.25 and 1.00, the AN improves the mAP of PD by 5.76%–8.00% for the $\mathcal{G}^{\text{a}}$ while the $\mathcal{P}_2^{\text{a}}$ remains at 30.65%, the $\mathcal{P}_4^{\text{a}}$ at 35.44%–35.98%, and the $\mathcal{P}_8^{\text{a}}$ at 7.34%–12.81%. The relative drop in the AUC of the PEL4VAD remains at 0.11%, 1.70% and 0.86% for the $\mathcal{G}^{\text{a}}$, $\mathcal{P}_2^{\text{a}}$ and $\mathcal{P}_4^{\text{a}}$, respectively. The $\mathcal{P}_8^{\text{a}}$ achieves a gain of 0.66%–0.77%. The α_l is employed for the bounded adaptive AN and has a pronounced impact for very large AN settings, i.e., $\mathbf{k}$ of $\mathcal{G}^{\text{a}}$ and $\mathbf{d}$ of $\mathcal{P}^{\text{a}}$, small α_l or/and target subjects with large surface area. We incorporated α_l into our algorithms for generalization, and it has a limited impact on cases with the lower base AN settings.

Fig. 18 illustrates different scaling functions, an alternative to the adaptive logarithmic function in Eq. (10). We have evaluated the AN and VAD performance on the $\mathcal{G}^{\text{a}}$ and $\mathcal{P}_2^{\text{a}}$. We kept the $\alpha_r = 1.0$ and $\alpha_l = 1.0$ for the experiment to focus the impact assessment on the functions. Table XI shows that the alternative functions achieve a gain close to the maximum AN, as they generate extremely high scaling scores (as shown in Fig. 18a).

We also normalized the maximum values of the functions to match the logarithmic function for fair comparison on the scaling curve structure (see Fig. 18b). Table XII shows a poor AN on the $\mathcal{P}_2^{\text{a}}$, gain of only 7.9%–15.81%, for the alternatives, while the logarithmic achieves better protection with a gain of 34.25%. The gain of the $f(x) = \ln(x)$ is due to the capability of allocating increased scaling (improving AN) for smaller subjects while damping the scaler for larger subjects. In contrast, the alternative $f(x)$s allocate higher leverage to larger subjects, whereas the smaller subjects in the video frames are barely anonymized. This leads to a leakage of privacy performance in the AN without a significant advantage over the non-adaptive AN.

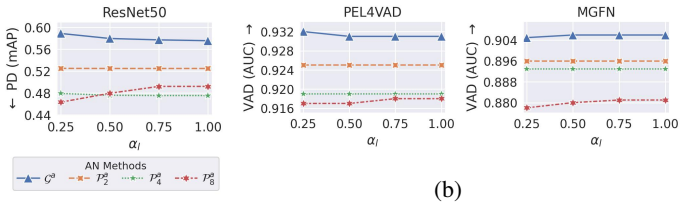

(a) (b)

Fig. 17: Performance evaluation on the hyperparameter α_l: a) PD on the VISPR Dataset [27], and b) VAD on XD-Violence Dataset [54]. Increasing the α_l improves the heavy AN with $\mathcal{P}_8^{\text{a}}$ and $\mathcal{G}^{\text{a}}$ in both the PD and VAD.

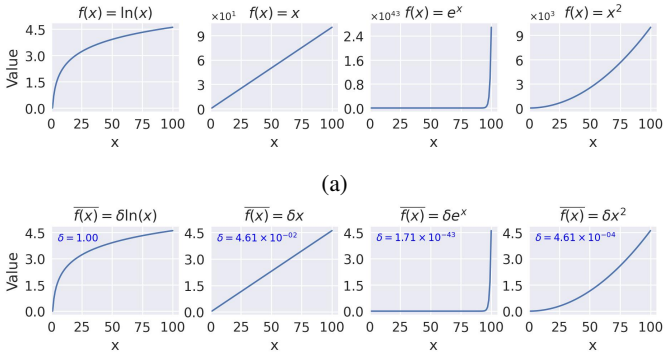

(a) (b)

Fig. 18: Scaling functions for the adaptive AN: (left to right) logarithmic ($f(x) = \ln(x)$), linear ($f(x) = x$), exponential ($f(x) = e^x$), and quadratic ($f(x) = x^2$). The $f(x)$ denotes the function in Eq. (10), where $x = \frac{100\|\mathbf{m_i}\|}{\|\mathbf{I}\|} \in (0, 100]$. The raw values are in (a) and normalized values (b), scaled by δ to match the range of $f(x) = \ln(x)$.

TABLE XI
ADAPTIVE SCALING FUNCTIONS: PD ON THE VISPR DATASET [27] AND VAD ON THE XD-VIOLENCE DATASET [54].

AN Method	$\text{mAP}_{\text{ResNet50}}\downarrow$	$\Delta_{\text{N}}\downarrow$	$\text{AUC}_{\text{PEL4VAD}}\uparrow$	$\Delta_{\text{N}}\uparrow$	$\text{AP}_{\text{PEL4VAD}}\uparrow$	$\Delta_{\text{N}}\uparrow$	$\text{AUC}_{\text{MGFN}}\uparrow$	$\Delta_{\text{N}}\uparrow$	$\text{AP}_{\text{MGFN}}\uparrow$	$\Delta_{\text{N}}\uparrow$
No-AN	0.797	–	**0.941**	–	**0.832**	–	**0.915**	–	**0.763**	–
$\mathcal{G}^0$	0.625	-21.58%	0.932	-0.96%	0.817	-1.80%	0.901	-1.53%	0.750	-1.70%
$\mathcal{G}^{\text{a}}(f(x) = \ln(x))$	0.575	-27.85%	0.931	-1.06%	0.819	-1.56%	0.906	-0.98%	0.759	-0.52%
$\mathcal{G}^{\text{a}}(f(x) = x)$	0.575	-27.85%	0.931	-1.06%	0.822	-1.20%	0.908	-0.77%	0.761	-0.26%
$\mathcal{G}^{\text{a}}(f(x) = e^x)$	0.575	-27.85%	0.932	-0.96%	0.822	-1.20%	0.908	-0.77%	0.759	-0.52%
$\mathcal{G}^{\text{a}}(f(x) = x^2)$	0.576	-27.73%	0.931	-1.06%	0.821	-1.32%	0.908	-0.77%	0.759	-0.52%
$\mathcal{G}^{\text{a}}_{\text{max}}$	0.540	-32.25%	0.933	-0.85%	0.822	-1.20%	0.910	-0.55%	0.753	-1.31%
$\mathcal{P}_2^0$	0.757	-5.02%	**0.941**	**0.00%**	**0.832**	**0.00%**	**0.915**	**0.00%**	**0.763**	**0.00%**
$\mathcal{P}_2^{\text{a}}(f(x) = \ln(x))$	**0.524**	**-34.25%**	0.925	-1.70%	0.802	-3.61%	0.896	-2.08%	0.729	-4.46%
$\mathcal{P}_2^{\text{a}}(f(x) = x)$	0.528	-33.75%	0.924	-1.81%	0.791	-4.93%	0.896	-2.08%	0.713	-6.55%
$\mathcal{P}_2^{\text{a}}(f(x) = e^x)$	0.535	-32.87%	0.932	-0.96%	0.819	-1.56%	0.906	-0.98%	0.745	-2.36%
$\mathcal{P}_2^{\text{a}}(f(x) = x^2)$	0.542	-31.99%	0.926	-1.59%	0.798	-4.09%	0.896	-2.08%	0.714	-6.42%
$\mathcal{P}^{\text{a}}_{\text{max}}$	0.533	-33.12%	0.931	-1.06%	0.816	-1.92%	0.909	-0.66%	0.751	-1.57%

Fig. 18a depicts the adaptive scaling functions, $f(x)$.

TABLE XII
ADAPTIVE SCALING FUNCTIONS (NORMALIZED): PD ON THE VISPR DATASET [27] AND VAD ON THE XD-VIOLENCE DATASET [54].

AN Method	$\text{mAP}_{\text{ResNet50}}\downarrow$	$\Delta_{\text{N}}\downarrow$	$\text{AUC}_{\text{PEL4VAD}}\uparrow$	$\Delta_{\text{N}}\uparrow$	$\text{AP}_{\text{PEL4VAD}}\uparrow$	$\Delta_{\text{N}}\uparrow$	$\text{AUC}_{\text{MGFN}}\uparrow$	$\Delta_{\text{N}}\uparrow$	$\text{AP}_{\text{MGFN}}\uparrow$	$\Delta_{\text{N}}\uparrow$
No-AN	0.797	–	**0.941**	–	**0.832**	–	**0.915**	–	**0.763**	–
$\mathcal{G}^0$	0.625	-21.58%	0.932	-0.96%	0.817	-1.80%	0.901	-1.53%	0.750	-1.70%
$\mathcal{G}^{\text{a}}(\overline{f(x)} = \ln(x))$	0.575	-27.85%	0.931	-1.06%	0.819	-1.56%	0.906	-0.98%	0.759	-0.52%
$\mathcal{G}^{\text{a}}(\overline{f(x)} = \delta f(x) = \delta x)$	0.579	-27.35%	0.933	-0.85%	0.819	-1.56%	0.903	-1.31%	0.752	-1.44%
$\mathcal{G}^{\text{a}}(\overline{f(x)} = \delta f(x) = \delta e^x)$	0.580	-27.23%	0.933	-0.85%	0.819	-1.56%	0.902	-1.42%	0.750	-1.70%
$\mathcal{G}^{\text{a}}(\overline{f(x)} = \delta f(x) = \delta x^2)$	0.579	-27.35%	0.933	-0.85%	0.819	-1.56%	0.903	-1.31%	0.752	-1.44%
$\mathcal{G}^{\text{a}}_{\text{max}}$	0.540	-32.25%	0.933	-0.85%	0.822	-1.20%	0.910	-0.55%	0.753	-1.31%
$\mathcal{P}_2^0$	0.757	-5.02%	**0.941**	**0.00%**	**0.832**	**0.00%**	0.915	0.00%	**0.763**	**0.00%**
$\mathcal{P}_2^{\text{a}}(\overline{f(x)} = \ln(x))$	**0.524**	**-34.25%**	0.925	-1.70%	0.802	-3.61%	0.896	-2.08%	0.729	-4.46%
$\mathcal{P}_2^{\text{a}}(\overline{f(x)} = \delta f(x) = \delta x)$	0.671	-15.81%	**0.941**	**0.00%**	0.831	-0.12%	**0.916**	**0.11%**	**0.763**	**0.00%**
$\mathcal{P}_2^{\text{a}}(\overline{f(x)} = \delta f(x) = \delta e^x)$	0.734	-7.90%	**0.941**	**0.00%**	**0.832**	**0.00%**	0.915	0.00%	0.762	-0.13%
$\mathcal{P}_2^{\text{a}}(\overline{f(x)} = \delta f(x) = \delta x^2)$	0.675	-15.31%	**0.941**	**0.00%**	**0.832**	**0.00%**	**0.916**	**0.11%**	**0.763**	**0.00%**
$\mathcal{P}^{\text{a}}_{\text{max}}$	0.533	-33.12%	0.931	-1.06%	0.816	-1.92%	0.909	-0.66%	0.751	-1.57%

Fig. 18b depicts the normalized adaptive scaling functions, $\overline{f(x)} = \delta f(x)$ where $\delta = \ln(100)/f(100)$.